J Mater Sci (2007) 42:8581–8591
DOI 10.1007/s10853-007-1851-z

Synthesis and characterization of porous κ-carrageenan/calcium phosphate nanocomposite scaffolds

Ana Luísa Daniel-da-Silva · Augusto B. Lopes · Ana M. Gil · Rui N. Correia

Received: 19 February 2007 / Accepted: 14 May 2007 / Published online: 10 July 2007

Abstract The polysaccharide κ-carrageenan was used in the production of macroporous composites containing nanosized hydroxyapatite, with potential application in bone tissue engineering. Biodegradable composite scaffolds were prepared combining in situ co-precipitation of calcium phosphates with a freeze-drying technique. The effect of the Ca/P molar ratio and total ceramic content on the chemical composition, microstructure and mechanical performance of the scaffolds were investigated by thermal analysis, X-ray diffraction, FTIR, transmission electron microscopy, scanning electron microscopy, He porosimetry and compressive tests. A mixture of amorphous calcium phosphates and/or nanosized calcium-deficient hydroxyapatite was obtained in most of the composites. The formation of hydroxyapatite was induced by higher Ca/P ratios, probably due to competing reticulation of the biopolymer with calcium cations. The composite scaffolds presented interconnected pores (50–400 μm) and porosity around 97% and calcium phosphates were uniformly dispersed in the κ-carrageenan matrix. Both microstructure and compressive mechanical properties of the scaffolds were affected by the ceramic content and, for a Ca/P molar ratio of 1.67, maximum compressive strength was achieved for a ceramic content of ca. 25 wt%. Above this value the structural integrity of the composite was damaged and a dramatic decrease in mechanical strength was verified. Compressive mechanical properties of the composites were improved by increasing Ca/P atom ratio.

A. L. Daniel-da-Silva (✉) · A. M. Gil
Department of Chemistry, CICECO, University of Aveiro, 3810-193 Aveiro, Portugal
e-mail: ana.silva@dq.ua.pt

A. B. Lopes · R. N. Correia
Department of Ceramics and Glass Engineering, University of Aveiro, 3810-193 Aveiro, Portugal

Introduction

Bone is one of the tissues with the highest demand for tissue reconstruction and bioresorbable scaffolds seeded with the appropriate type of cells should provide templates for tissue regeneration. Natural bone tissue is a composite material that comprises an organic phase (collagen) and a mineral phase mainly composed of hydroxyapatite (HAP). Synthetic HAP has been intensively investigated as the inorganic component of scaffold materials for bone tissue engineering, due to its high biological affinity to living bone [1–3]. It can bind chemically to the surrounding tissues and is non-toxic, non-inflammatory, non-immunogenic, osteoconductive and may increase the rate of bone regeneration [4–6]. However, pure, stochiometric and dense HAP is one of the least degradable forms of calcium phosphates [7] and its application is limited due its brittleness. Often, other more soluble calcium phosphates are preferred as bone-substitute materials such as non-stochiometrical HAP, β-tricalcium phosphate (β-TCP) and amorphous calcium phosphates [8–11].

In the past few years several attempts have been made to mimic bone properties and structure by using polymer/ceramic composite materials [1]. The composite is expected to have improved mechanical properties compared to the neat polymer and better structural integrity and flexibility than the brittle ceramics. Synthetic polymers like polylactic acid (PLA), polyglycolic acid (PGA) and their different copolymers (poly(lactic-*co*-glycolic acid)—PLGA) have

been widely investigated in this field [12, 13]. Naturally derived polymers such as collagen, gelatine, alginate and chitosan have also been studied [14–17].

This paper describes the use of κ-carrageenan in the preparation of HAP-containing composites for tissue engineering purposes. κ-carrageenan is a linear sulfated polysaccharide extracted from red seaweeds. It has a basic linear primary structure based on a repeating disaccharide unit of α(1–3)-D-galactose and β(1–4)-3,6-anhydro-D-galactose and contains one sulphate group per disaccharide unit at carbon 2 of the 1,3 linked galactose unit (Fig. 1). The solution of κ-carrageenan may form strong thermally reversible gels upon cooling in the presence of specific cations such as potassium, sodium or calcium [18–20]. It is used as an important gelling agent in the food and pharmaceutical industries, mainly due to its non-toxicity and water-solubility [21]. In addition, this polysaccharide degrades in the body to non-harmful and non-toxic compounds. Therefore, a composite of hydroxyapatite and κ-carrageenan is expected to accomplish the requirements of bioresorbality and biocompatibility for scaffold materials. Despite its potential, a limited number of applications of κ-carrageenan are found and these include a number of biomedical applications such as microencapsulation and immobilization of drugs [22–24] and wound dressing [25].

The preparation of HAP-containing composites can be carried out either by precipitating HAP crystals within the polymeric matrix or by using the conventional mixing technique. Recently, nano-level HAP has been demonstrated as having a good impact on cell–biomaterial interaction [26, 27], stimulating osteoblast activity and adhesion and, therefore, leading to enhanced bone growth. The in situ co-precipitation process has been reported to be efficient in obtaining nanosized HAP particles in other polymeric systems [17, 28].

In the present study porous scaffolds were prepared by a co-precipitation method using calcium acetate, ammonium di-hydrogen phosphate and κ-carrageenan as starting materials. The effect of the Ca/P molar ratio of reactants and inorganic fraction of the composite on the properties of scaffolds was investigated. These properties included the inorganic phase obtained, crystallite size, porosity and morphology of the scaffolds and compressive mechanical performance.

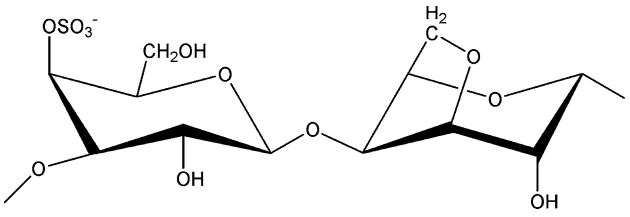

Fig. 1 Structural disaccharide unit of κ-carrageenan

Experimental

Materials

κ-carrageenan (Fluka Chemie, Denmark, Batch No. 442129) was used as received. The average molecular weight (M_W) of the polymer was 300,000 and was obtained from intrinsic viscosity measurements using the Mark–Houwink relation, $[\eta]$ (mL/g) = K · M_W^{α} (K = 3.11 × 10^{-3}, α = 0.95) in 0.1 M NaCl aqueous solution as described elsewhere [29]. To prepare the solutions used to measure viscosity, κ-carrageenan was converted to its sodium salt [30]. Chemicals used in this investigation were $Ca(CH_3COO)_2$ (>93%, Riedel-deHaën, Germany), $NH_4H_2PO_4$ (Panreac, Spain) and ammonia solution 25% (Riedel-deHaën, Germany). All chemicals were used as received without further purification.

Synthesis of composites

A κ-carrageenan aqueous solution was prepared by dissolving κ-carrageenan (κ-CRG) powder into boiling distilled water to a concentration of 20 g/L. Under stirring, a $Ca(CH_3COO)_2$ aqueous solution (0.7 M) was slowly added to 25 mL of the κ-CRG solution, followed by the addition of $NH_4H_2PO_4$ solution (0.5 M). Subsequently, ammonia solution was added dropwise in order to obtain a final pH between 9 and 10. Each synthesis was performed at 80 °C, under reflux and magnetic stirring at 500 rpm for a period of 3 h. At the final stage, the system was left open with the purpose of evaporating the excess of water. The final volume of the solution was 25 mL.

Gel formation was induced by cooling to room temperature and samples were frozen at –18 °C for a period of 8 h. The frozen composites were then lyophilized (freeze-dryer model Lyph Lock 4.5, Labconco) at a freeze-drying temperature and vacuum of –50 °C and 15 × 10^{-3} mbar, respectively for a period of 3 days. The lyophilization is one of the most common methods to induce porosity in the scaffolds [31, 32] and consists in a vacuum–drying process during which ice crystals are sublimated, leaving behind the polymer as a foam. Afterwards the scaffolds were cut to make cylindrical specimens for mechanical testing.

Different composites were prepared by changing the molar ratio Ca/P and the weight fraction of calcium phosphate (CP) (Table 1).

Some compositions were further calcined at 900 °C, in air, for characterization purposes and confirmation of data obtained in as-synthesized material.

Table 1 Composition of κ-CRG:CP composite samples

κ-CRG:CP (wt%)	Ca/P	$Ca(CH_3COO)_2$ (mmol)	$NH_4H_2PO_4$ (mmol)
75:25	1.67	1.7	1.0
50:50	1.67	5.0	3.0
25:75	1.67	14.9	9.0
50:50	1.80	5.0	2.8
50:50	1.90	5.0	2.6

Characterization of κ-CRG:CP composites

κ-CRG:CP composites were characterized by thermogravimetry in air between 25 °C and 900 °C at a heating rate of 10 °C/min (Shimadzu TGA-50). The purpose was to assess thermal stability and to confirm the actual composition of the composites.

Fourier transform infra-red spectroscopy (FTIR) was used to characterize the composites. FTIR spectra were collected using a spectrometer Mattson 7000 and a horizontal attenuated total reflectance (ATR) cell, using 128 scans at a resolution of 4 cm^{-1}.

X-ray diffraction analysis (XRD) was used to characterize the crystallinity, phase composition and structure of the materials. XRD experiments were performed on composites before and after being calcined at 900 °C, with an X-ray difractometer (Rigaku Geigerflex Dmax-C) using a monochromatic Cu Kα radiation. The average size (L) of the HAP crystallites was calculated from XRD patterns, using Scherrer's equation [33],

$$L = \frac{K\lambda}{\beta_m \cos\theta} \quad (1)$$

where β_m is the peak width at half of the maximum intensity (rad), λ the wavelength of X-ray radiation (1.54178 Å) and K is a constant related to the crystallite shape, approximately equal to unity. The HAP average crystallite size was calculated based on the broadening of (002) reflection peak at $2\theta = 26°$. The experimental broadening of the reflection peak (β^*) fitted by a Gaussian function is expressed as the sum of two main contributions, the crystallite size contribution (β_m) and the instrumental broadening contribution (β_{inst}). The average crystallite size contribution is obtained according to Eq. 2.

$$\beta_m = \beta^* - \beta_{inst} \quad (2)$$

The crystallinity degree (X_c), defined as the fraction of crystalline phase present in the examined volume, can be also calculated from the peak width using the Eq. 3,

$$X_c(\%) = \left(\frac{K_A}{\beta_m}\right)^3 \times 100 \quad (3)$$

where K_A is a constant set at 0.24 [34] and β_m is given in degrees.

Transmission electron microscopy (TEM) was used to determine the size of calcium phosphate particles. Samples were prepared by evaporating dilute ethanol suspensions on a copper grid coated with an amorphous carbon film and the experiments were performed on a JEOL 200CX microscope operating at 300 kV.

The porosity of the scaffolds was assessed with a helium pycnometer Quantachrome model MVP-1 (Quantachrome Instruments, USA). The ratio between real density d_{real}, measured in the He pycnometer, and geometric density d_{geom} (ratio of sample weight to sample volume) measures the porosity (Eq. 4) [35].

$$\%\text{porosity} = \left(1 - d_{geom}/d_{real}\right) \times 100 \quad (4)$$

The morphology of the scaffolds was examined with a scanning electron microscope (Hitachi S-4100, Japan) at an accelerating voltage of 25 kV, using gold-sputtered samples.

The compressive mechanical tests were performed on cylindrical specimens of approximately 20 mm diameter and 5 mm length, on a texturymeter TA-HDI (Stable Microsystems Ltd), using 0.2 mm/s as crosshead speed. The compressive strength ($\sigma_{30\%}$) was determined at a nominal strain of 0.3. The elastic modulus was calculated as the slope of the initial linear portion of the stress–strain curve.

Results and discussion

Chemical composition of composites

Figure 2 shows the thermogravimetric curves of pure κ-CRG and κ-CRG:CP composites, as well as the curve for HAP prepared in absence of biopolymer, for a molar ratio Ca/P = 1.67 (HAP 1.67). κ-carrageenan decomposed fast at 250 °C and further decomposition occurred in three steps, with rate maxima around 327°, 430° and 526 °C. When heated up to 900 °C, HAP 1.67 showed a weight loss in three stages. The first stage, up to 200 °C, corresponds to the vaporization of adsorbed water on the surface of HAP, while the second (220–400 °C) is due to the vaporization of the water of crystallization of HAP and the third stage (400–565 °C) might be due to loss of carbonate that eventually was incorporated in the calcium phosphate structure during the synthesis [36–40].

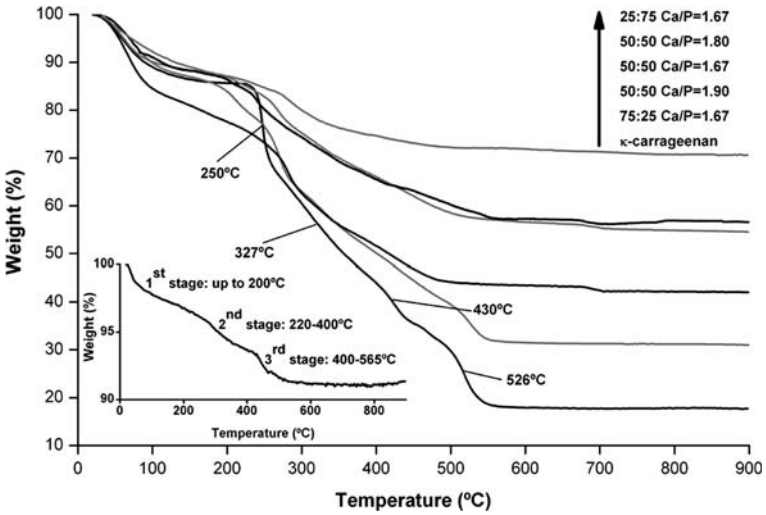

Fig. 2 Thermogravimetric curves of pure κ-carrageenan and κ-CRG:CP composites (outer graph). The inner graph shows the thermogravimetric curve of HAP (Ca/P = 1.67)

In general, composites show increased thermal stability compared to κ-CRG, since the onset of the main decomposition step (around 250 °C) increases, with exception of the sample containing less inorganic phase. The improvement of thermal stability of the composites with increasing HAP content was also observed in other HAP-containing systems such as polyamide/nano-HAP composites and was attributed to the formation of hydrogen bonds between the matrix and HAP [39]. Table 2 lists the expected and experimentally determined final weight at 900 °C of the composites. The expected final weight of the composites was calculated taking into account the residue obtained for the pure κ-CRG and HAP 1.67. The general agreement between experimental and expected values is clear and the differences observed arising possibly from variations in moisture uptake of the scaffolds before thermogravimetric analysis.

Figure 3 shows the FTIR-ATR spectra of κ-carrageenan and κ-CRG:CP composite samples. The main bands arising from κ-carrageenan are located at 3,000–3,500 cm^{-1} (O–H stretching), 1,225 cm^{-1} (S–O asymmetric stretching), 1,040–1,070 cm^{-1} (C–O and C–OH stretching), 920 cm^{-1} (C–O–C stretching in 3,6-anhydrogalactose) and 845 cm^{-1} (C–O–S stretching in α(1–3)-D-galactose) in agreement with the literature [41].

Table 2 Thermogravimetric data of composites

κ-CRG:CP (wt%)	Ca/P	Experimental final weight (%)	Expected final weight (%)
100:0	–	17.7	–
0:100	1.67	91.4	–
75:25	1.67	31.0	36.1
50:50	1.67	54.5	54.5
25:75	1.67	70.6	73.0
50:50	1.80	56.6	54.5
50:50	1.90	51.0	54.5

FTIR-ATR spectra of composites are similar and show typical absorption bands of HAP: $v_3(PO_4^{3-})$ at 1,045–1,092 cm^{-1} and $v_1(PO_4^{3-})$ symmetric stretch between 900 cm^{-1} and 1,100 cm^{-1} that overlap C–O and C–OH stretching bands from κ-carrageenan, $v_2(PO_4^{3-})$ at 474 cm^{-1}, and $v_4(PO_4^{3-})$ bending between 550 cm^{-1} and 650 cm^{-1} [42, 43]. As expected, the relative intensity of the absorption band $v_4(PO_4^{3-})$ becomes higher as the ceramic content increases. It is interesting to note that composites show broadening of the O–H stretching band and shiftning to lower wavenumbers, compared to pure κ-carrageenan. This may be due to the formation of hydrogen bonds between the polysaccharide hydroxyl groups (–OH) and HAP, which is in agreement with thermogravimetry results. Carbonate groups, which have a typical band at 1,410–1,415 cm^{-1}, have been found present in the κ-CRG:CaP composites, suggesting that calcium phosphate may form with some carbonate incorporation [17]. However, this band, together with the absorption band at 1,540 cm^{-1} might also be attributed to stretching vibrations of the acetate group [44].

Figure 4 shows the XRD patterns of pure κ-carrageenan and some of the composites, before and after calcination.

κ-carrageenan produces a diffuse diffraction pattern indicating that the molecules of this polysaccharide do not organize into microcrystallites. Poorly crystalline HAP was identified as the only crystalline phase in the scaffolds. However, after being calcined, the XRD pattern of most of the composites shows a second crystalline phase suggested to correspond to β-$Ca_3(PO_4)_2$ (β-TCP). β-TCP does not form in aqueous systems under normal laboratory conditions, i.e., up to 100 °C and at atmospheric pressures [37]. Therefore, the β-TCP phase identified in the calcined composites must be a calcination product of amorphous

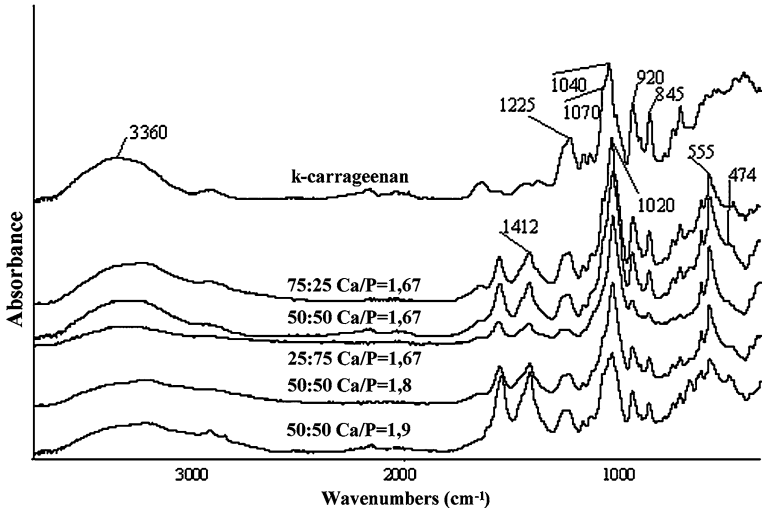

Fig. 3 FTIR-ATR spectra of κ-carrageenan and κ-CRG:CP composites

calcium phosphate (ACP) produced during the synthesis. Indeed, ACP often occurs as a transient phase during the formation of calcium phosphates in aqueous systems, particularly when the Ca/P atom ratio is lower than the stoichiometric value of 1.67, and may crystallize β-TCP above 650 °C [37]. Another possible explanation is that calcium-deficient hydroxyapatite is being formed during the synthesis, although we could not identify the HPO_4^{2-} typical bands in the infra-red spectra of the composites. On heating above 700 °C dry Ca-deficient hydroxyapatite with a molar ratio Ca/P between 1.5 and 1.67 will convert into a mixture of HAP and β-TCP [45].

For the highest Ca/P molar ratio tested (1.9), no relevant β-TCP reflection peaks were detected in the calcined composite, which indicates the absence of significant amounts of ACP or the preparation of an hydroxyapatite close to the stoichiometric Ca/P ratio In absence of polysaccharide, analogous results were obtained when the synthesis was performed at a Ca/P molar ratio of 1.67. These results suggest that κ-CRG inhibits the formation of HAP. It is well known that monovalent and divalent cations, such as Ca^{2+}, have a pronounced effect in the gelling process of κ-carrageenan [18, 19, 30]. Gelation of κ-carrageenan is a thermoreversible process that consists in the formation of double helical conformations followed by aggregation of helices (Fig. 5). At high temperatures a random coil conformation is obtained (sol); with decreasing temperature, random coils become helices, which subsequently aggregate to form junction zones of gel [21, 46].

In general, added cations increase the stability of the ordered conformation (double helix) and promote gelation, the nature of the cation–biopolymer interaction depending on the ion. For instance, Na^+ and Li^+ seem to play a purely electrostatic effect while K^+, Rb^+ and Cs^+ have been shown to specifically bind to the helical structure [21, 47, 48]. Divalent cations such as Ca^{2+} affect the sol–gel transition primarily by electrostatic interactions, by shielding the charge of sulfate groups [18, 21]. Therefore, in the presence of the κ-carrageenan, part of the added Ca^{2+} ions should participate in the conformational stabilization, thus reducing the bulk Ca/P molar ratio. As a result, poorly Ca-deficient HAP and/or ACP are probably formed. Typically, the Ca/P molar ratio of Ca-deficient HAPs may vary from 1.5 to 1.67, while for the precipitation of ACP in aqueous medium lower values are needed, e.g., between 1.18 and 1.5 [37, 45]. These results suggest that Ca^{2+} ions that take part in gel cross-linking become unavailable for the formation of calcium phosphates. One possible reason is that the stereo-chemical geometry of the double helical ordered conformation might be incompatible with the tetrahedral structure of phosphate anions. Under these conditions, the nucleation of a solid phase of calcium phosphate coordinated to the polysaccharide is certainly more difficult.

In order to characterize the composite materials further, the average size (L) of the HAP crystallites and the crystallinity degree (X_c) were calculated from XRD patterns, as described in the experimental section. Table 3 summarizes the crystallinity degree of the composites and the average HAP crystallite size, with exception to the composite containing 25 wt% of calcium phosphates as the reflection peak at $2\theta = 26°$ can hardly be distinguished.

κ-CRG:CP composites exhibit a low degree of crystallinity and HAP average particle size is between 15 nm and 18 nm in diameter. The results obtained show no systematic effect of the ceramic content and Ca/P ratio on HAP crystallite size. Nevertheless, the average crystallite size of HAP obtained under the same conditions but in absence of κ-CRG was around 43 nm and 36 nm for Ca/P = 1.67 and Ca/P = 1.9, respectively. Therefore, the presence of κ-CRG in the system seems to have an inhibitory effect on the crystal growth of HAP.

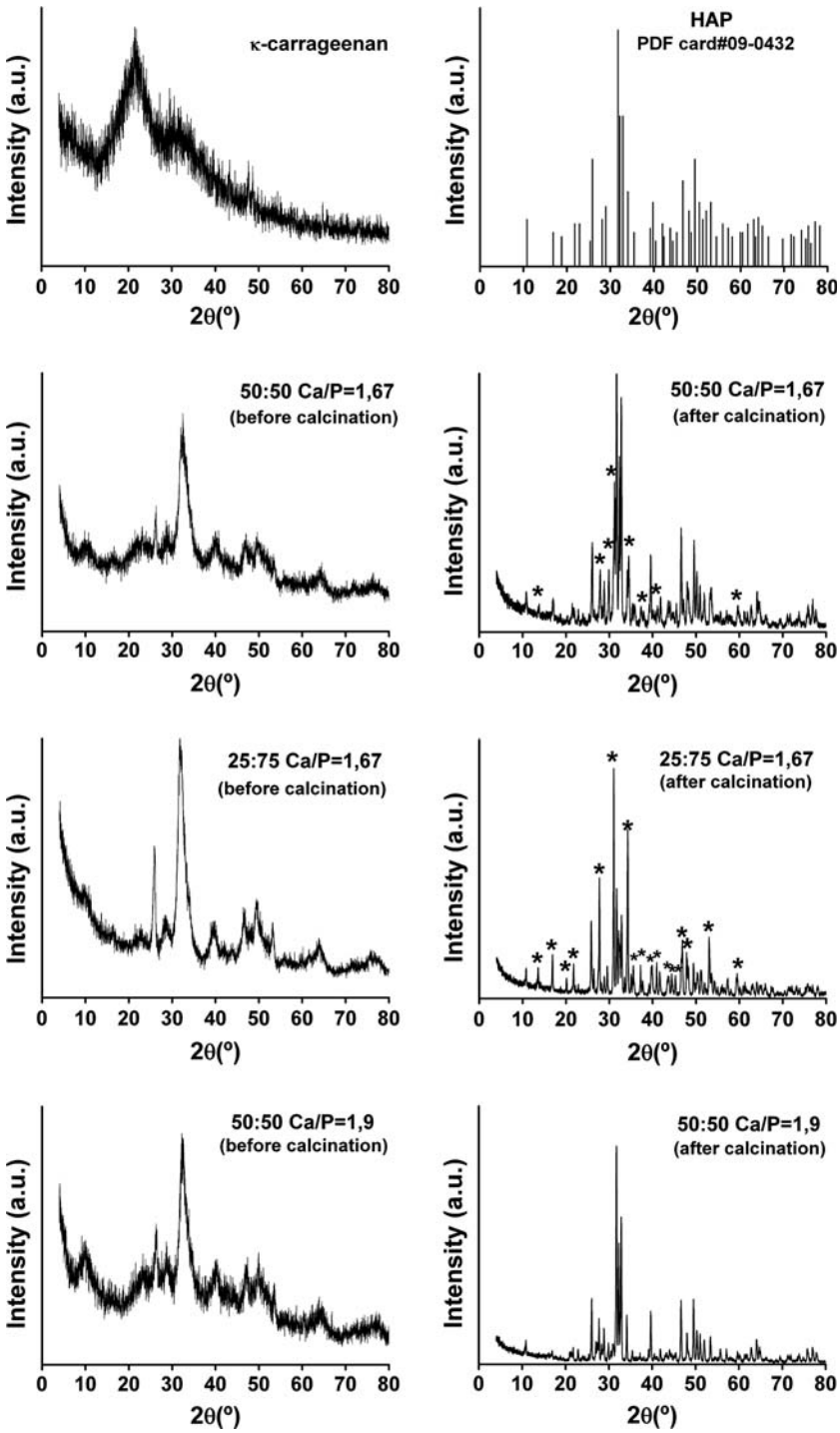

Fig. 4 XRD patterns of composites before and after calcination. Reflections originating from hydroxyapatite are unmarked while reflections corresponding to β-TCP are indicated with * (pdf card #09-0169)

Figure 6 shows the morphology of HAP crystals prepared without biopolymer (Ca/P = 1.67), before and after calcination, and of the composite 50:50 (Ca/P = 1.9) after calcination, confirming that nanosized HAP is obtained in the synthesis of composites (TEM observation of individual HAP crystals in the composite before calcination was unsuccessful due to agglomeration). The shape of non-calcined HAP crystals (Fig. 6a) is characteristically needlelike with size around 180 nm × 6 nm while calcined HAP (Fig. 6b) exhibits platelike shapes of size around 130 nm × 60 nm. Platelike HAP crystals with 300 nm × 100 nm are present in the calcined composite (Fig. 6c). The particle size measured by TEM is significantly higher than the average size estimated using Scherrer's equation. Differences observed may be due in part to the assumption of spherically shaped particles, not corroborated by TEM

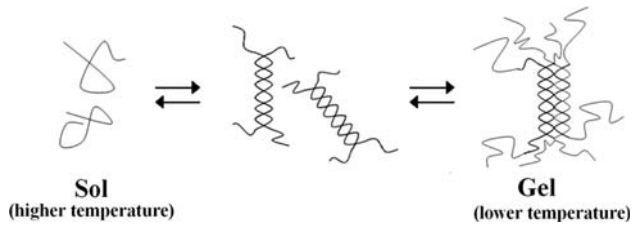

Fig. 5 Schematic gelation mechanism of the κ-carrageenan in aqueous media (adapted from reference [42])

Table 3 Average crystallite size of HAP and crystallinity degree (X_c) of the composites, determined by XRD, and porosity of the scaffolds measured with a helium pycnometer

κ-CRG:CP (wt%)	Ca/P	L (nm)	X_c (%)	Porosity (%)
100:0	–	–	–	97.3
75:25	1.67	–	–	96.9
50:50	1.67	16.5 ± 5.0	6.6	97.4
25:75	1.67	18.3 ± 3.1	8.6	96.9
50:50	1.80	16.2 ± 3.6	6.4	96.5
50:50	1.90	14.6 ± 5.2	6.3	96.9

analysis. Moreover, X-ray diffraction is sensitive to coherent scattering domains, whose size can significantly differ from that of the particles in the case where lattice defects or amorphous surface layers are present [49].

Scaffold morphology and mechanical properties

Both carrageenan-only and composite scaffolds show a continuous structure of irregular pores and good interpore connectivity (Fig. 7). The pore size of pure carrageenan scaffold ranges from several microns up to about 600 microns and decreases with increasing amounts of the inorganic fraction. Pore walls become thicker and better defined as the inorganic content increases as a result of the incorporation of larger amounts of ceramic filler in the walls (Figs. 7, 8). In the composites containing 50 wt% inorganic fraction, pore size ranges from about 50 μm to 300 μm for Ca/P = 1.67 and increases with increasing Ca/P molar ratio up to around 400 μm for Ca/P = 1.9 (Fig. 7c, e, respectively). When the polymer/inorganic ratio is higher than 1:1, the pore structure becomes more and more irregular and the average pore size seems to increase. Similar trends have been observed in HAP-polylactic acid [50] and HAP-alginate [51] composites. Additionally, nanoporous walls are observed in the composite containing 75 wt% inorganic fraction (Fig. 8c).

The average porosity of pure κ-CRG and composite scaffolds is around 97% (Table 3) and no influence of the ceramic content and Ca/P ratio on the porosity was found. The compressive stress–strain diagrams for pure κ-carrageenan and for κ-carrageenan/CP scaffolds are included in Fig. 9. The linear regime in the stress–strain curves is indicative of the elastic behavior of the scaffold and was taken as reference for the calculus of Young's moduli. After this linear regime the stress sensitivity to strain decreases, probably as a result of cellular collapse or cell wall buckling. Pure carrageenan scaffolds are soft, spongy and very flexible, with a maximum strain of around 25% before loss of elasticity. For Ca/P = 1.67 composites the addition of 25 wt% of ceramic filler clearly increases stiffness and improves strength, but higher ceramic

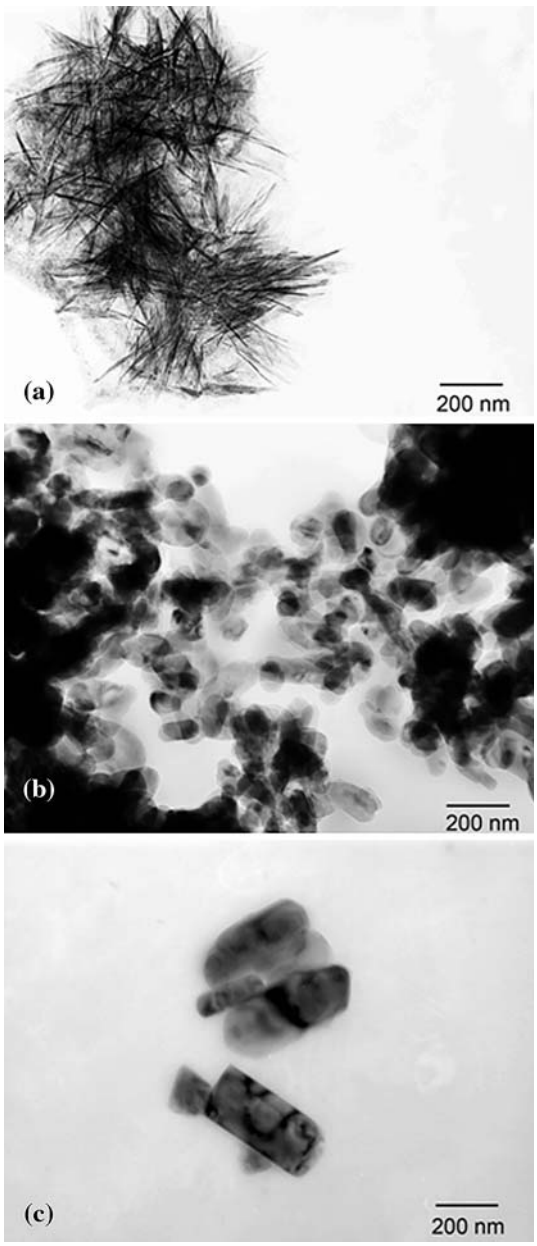

Fig. 6 TEM images of HAP (Ca/P = 1.67) before (**a**) and after calcination (**b**) and (**c**) composite 50:50 (Ca/P = 1.9) after calcination

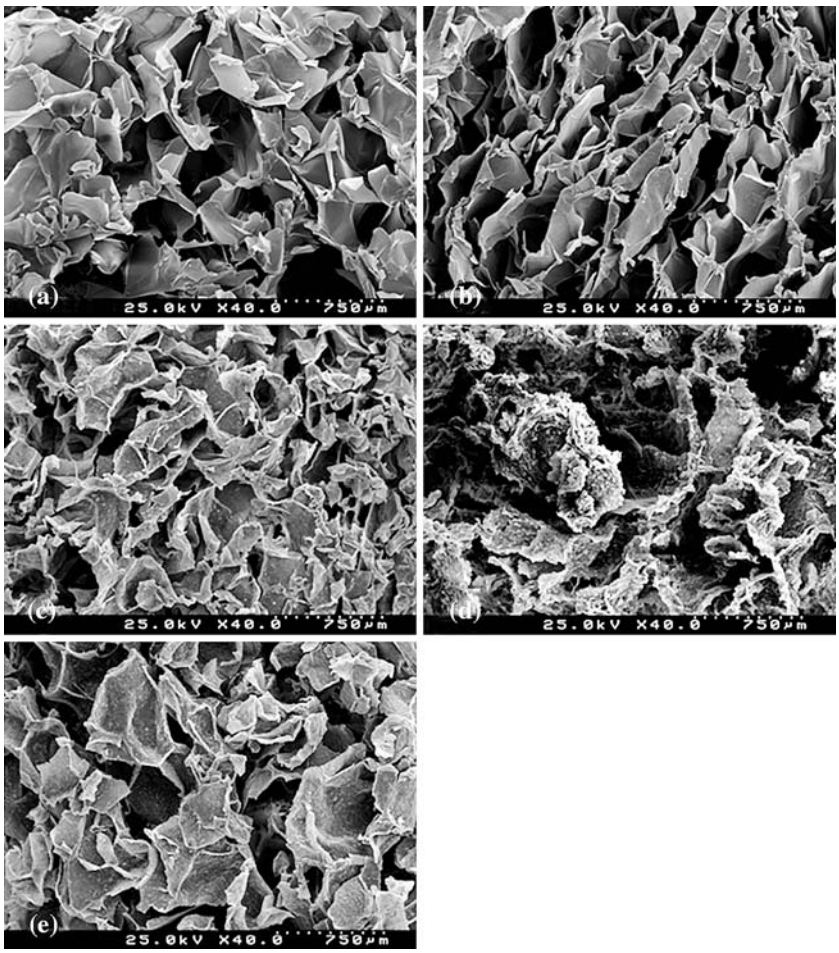

Fig. 7 SEM images of porous scaffolds, original magnification 40×: (**a**) κ-carrageenan; (**b**), (**c**) and (**d**) were prepared with a Ca/P molar ratio of 1.67, with 25, 50 and 75 wt% inorganic fraction, respectively; (**e**) composite 50 wt% Ca/P = 1.9

contents bring the compressive strength and stiffness back to lower values, down to those for κ-carrageenan. In any case, however, composites exhibit higher strengths than the matrix beyond the linear limit. Also, increasing the Ca/P ratio for 50 wt% of inorganic content leads to a progressive improvement in compressive strength.

Figure 10 shows the influence of the inorganic fraction and Ca/P molar ratio on the compressive strength ($\sigma_{30\%}$) and compressive modulus of the composites. The values obtained are of the same order of magnitude as those reported for other polysaccharide-based scaffolds [9, 10].

As mentioned before, for a Ca/P ratio of 1.67 the compressive properties of κ-CRG improve with the incorporation of up to 25 wt% of calcium phosphates but worsen for higher ceramic contents. Although thicker pore walls should contribute to the improvement of mechanical properties, it is believed that above a certain amount the precipitating calcium phosphates may interfere with the gelation mechanism of κ-carrageenan and the rheological properties of the resultant gel should deteriorate. These results are consistent with a previous study of the structure of calcium-induced κ-CRG gels showing that there is a calcium-carrageenan ratio that optimizes the strength of the gel. Increasing this optimum concentration, the network structure coarsens and elastic moduli decrease [30].

The results obtained for compressive modulus are in harmony with SEM observations. As mentioned before, the scaffold microstructure becomes more irregular for a ceramic content higher than 25 wt% (Fig. 7b). In a reported work about the precipitation in situ of nano-hydroxyapatite on a chitosan matrix [11] a similar result was found, the maximum value of compressive strength corresponding to 30 wt% HAP. In addition, an improvement of the compressive mechanical properties is observed as the Ca/P ratio increases, such conditions corresponding to a decrease in the fraction of amorphous phase, as observed by XRD. This is consistent with previous observations that higher crystallinity tends to induce higher mechanical values [1].

Potential applications of the scaffolds

The composites prepared in this study fulfill some of the requirements of scaffold materials for bone regeneration

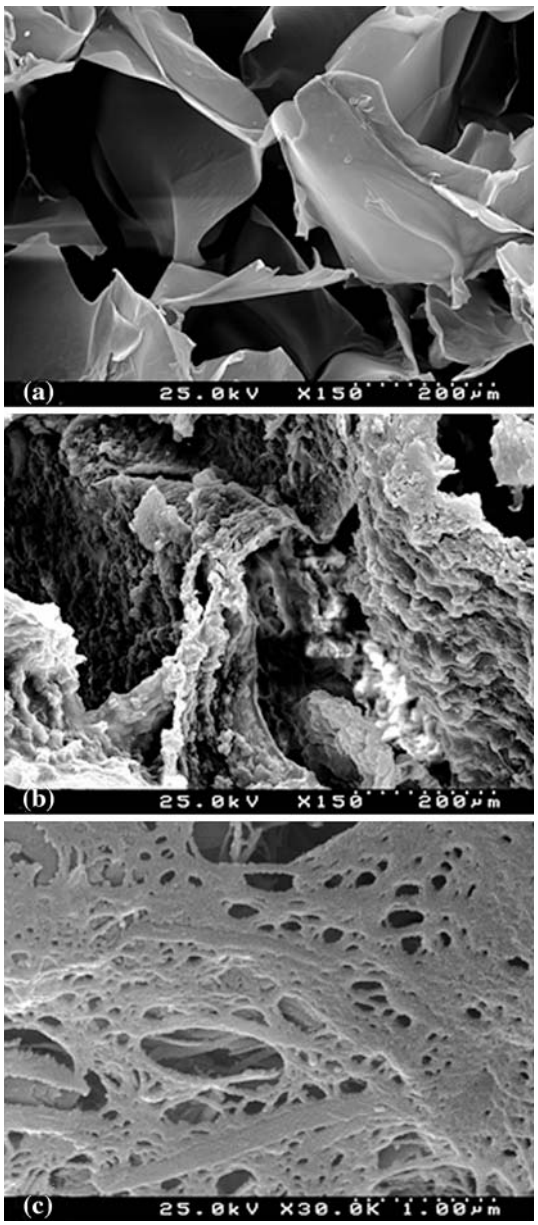

Fig. 8 SEM images of porous scaffolds. Original magnifications: (**a**) κ-carrageenan 150×; (**b**) 25:75 Ca/P = 1.67 150×; (**c**) 25:75 Ca/P = 1.67 30,000×

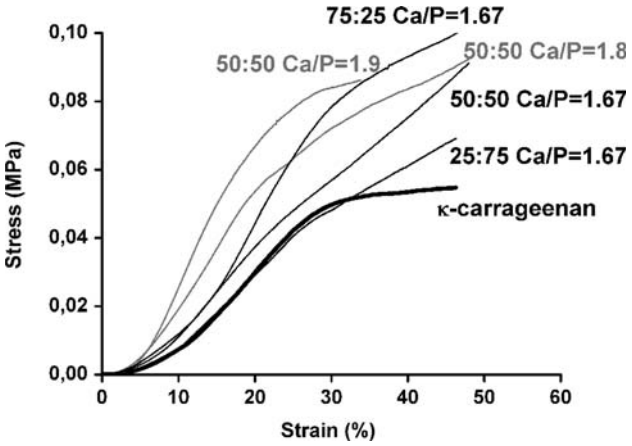

Fig. 9 Stress–strain curves of pure κ-carrageenan and of κ-CRG:CP composites

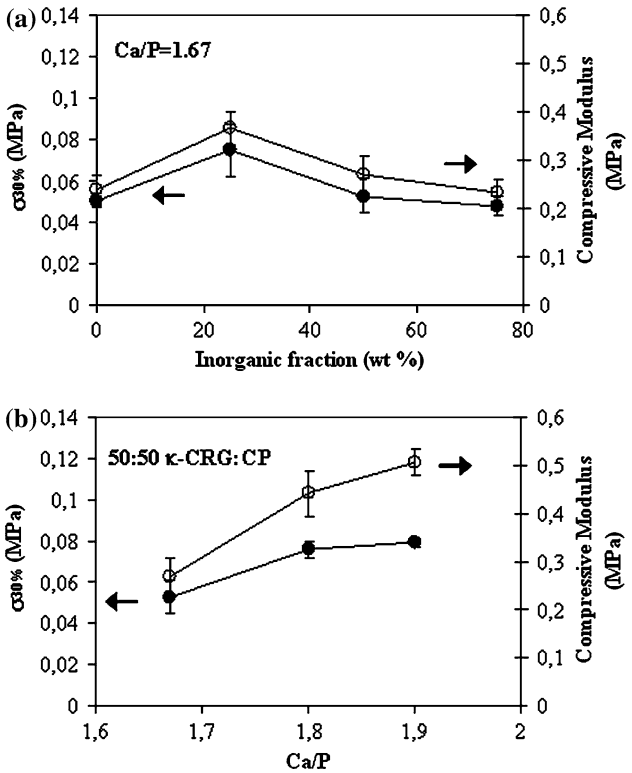

Fig. 10 Compressive strength and compressive modulus of the composites: (**a**) effect of the inorganic fraction (Ca/P = 1.67); (**b**) effect of Ca/P ratio (50:50) (● compressive strength; ○ compressive modulus)

since they exhibit interconnected porosity above 90% and pore diameter larger than 100 μm, which are compulsory for cell penetration and proper vascularization of the in-grown tissue [1]. The low degree of HAP crystallinity in the composites might be also advantageous since previous works have shown that the rate of new bone formation coincides more closely with the resorption rate of poorly crystalline or amorphous calcium phosphate ceramics [52, 53]. Additionally, calcium phosphate nanoparticles seem to be uniformly distributed in pore walls and the resulting surfaces may provide a particularly suitable environment for osteoblast attachment and growth. Nevertheless, although coherent with other polysaccharide composites the compressive performance of these composites is still modest when compared to the natural bone. Trabecular bone exhibits values ranging between 5–10 MPa and 50–100 MPa for compressive strength and Young modulus, respectively, depending on its density [54, 55]. Some strategies to overcome the weak mechanical properties of

these composites might be to blend it with a homopolymer or a compound that can be polymerized in situ. Regarding the latter for instance, it has been reported that the addition of diallyldimethylammonium and its subsequent photopolymerization allows the preparation of κ-carrageenan based hydrogels with remarkably better gel strength than the pure κ-carrageenan gel [56]. Although these improvements, mechanical properties close to those of the natural bone hardly would be achieved and limit the usage of these composites to non-load-bearing bone applications. They can be placed into critical defects in a minimally invasive manner to promote regeneration, which could not otherwise occur.

Conclusions

Porous nanocomposites were successfully prepared by co-precipitation of calcium phosphates into κ-carrageenan, followed by thermally induced gelification and freeze-drying. For a precursor Ca/P molar ratio of 1.9 only nanosized hydroxyapatite was detected while below this value nanosized Ca-deficient hydroxyapatite and/or amorphous calcium phosphates were obtained, which suggests that part of the calcium ions are captured by the polysaccharide in its gelation process, becoming unavailable for the formation of hydroxyapatite. The porosity and morphology of the composites was adequate to their application in bone tissue engineering. Both microstructure and compressive mechanical properties of the scaffolds were found to be affected by the calcium phosphate content. The higher the total inorganic content, the thicker the pore walls and the lower the pore size of the composites. The compressive mechanical properties of the scaffolds exhibit a maximum for a certain ceramic content. Above this value the structural integrity of the composite is progressively lost and a decrease in mechanical strength is observed. The compressive mechanical performance of the scaffolds, although similar to other polysaccharide based systems is still modest for bone engineering components and in the future further efforts will be pursued in order to improve it.

Acknowledgements The help of Dr. J. A. T. Lopes da Silva in the execution of the compressive mechanical tests and of Dr. D. Evtyugin in the determination of molecular weight of κ-carrageenan are gratefully acknowledged. A. L. Daniel da Silva thanks CICECO-Centro de Investigação em Materiais Cerâmicos e Compósitos, University of Aveiro, Portugal, for funding this work.

References

1. Rezwan K, Chen QZ, Blaker JJ, Boccaccini AR (2006) Biomaterials 27:3413
2. Knowles JC (2003) J Mater Chem 13:2395
3. Legeros RC (1991) In: Calcium phosphate in oral biology and medicine, vol 15. Karger, New York
4. Ogiso M (1998) J Biomed Mater Res B 43:318
5. Hench LL (1991) J Am Ceram Soc 74:1487
6. Habal MB (1991) J Craniofac Surg 2:27
7. Klein CPAT, de Blieck-Hogerworst JMA, Wolke JGC, de Groot K (1990) Biomaterials 11:509
8. Yin Y, Ye F, Cui J, Zhang F, Li X, Yao K (2003) J Biomed Mater Res A 67:844
9. Zhao L, Chang J (2004) J Mater Sci-Mater M 15:625
10. Araújo JV, Lopes-da-Silva JA, Almeida MM, Costa MEV (2006) Mater Sci Forum 514–516:1005
11. Li Z, Yubao L, Aiping Y, Xuelin P, Xuejiang W, Xiang Z (2005) J Mater Sci-Mater M 16:213
12. Tormala P, Vainiopa S, Kilpikari J, Rokkanen P (1987) Biomaterials 8:42
13. Murphy WL, Kohn DH, Mooney DJ (2000) J Biomed Mater Res A 50:50
14. Du C, Cui FZ, Zhu XD, de Groot K (1999) J Biomed Mater Res A 44:407
15. Yaylaoglu MB, Korkusuz P, Ors U, Korkusuz F, Hasirci V (1999) Biomaterials 20:711
16. Lin H-R, Yeh YJ (2004) J Biomed Mater Res B 71B:52
17. Kong L, Gao Y, Cao W, Gong Y, Zhao N, Zhang X (2005) J Biomed Mater Res A 75:275
18. Lai VMF, Wong PA-L, Lii C-Y (2000) J Food Sci 65:1332
19. Michel A-S, Mestdagh MM, Axelos MAV (1997) Int J Biol Macromol 21:195
20. Mangione MR, Giacomazza D, Bulone D, Martorana V, Cavallaro G, San Biagio PL (2005) Biophys Chem 113:129
21. Piculell L (1995) In: Food polysaccharides and their applications. Marcel Dekker Incorporation, New York, pp 205–217
22. Garcia AM, Ghaly ES (1996) J Control Release 40:179
23. Bornhöft M, Thommes M, Kleinebudde P (2005) Eur J Pharm Biopharm 59:127
24. Naim S, Samuel B, Chauhan B, Paradkar A (2004) AAPS Pharm Sci Tech 5(2):article 25
25. Sen M, Avci EN (2005) J Biomed Mater Res A 74:187
26. Webster TJ, Ergun C, Doremus RH, Siegel RW, Bizios R (2000) Biomaterials 21:1803
27. Balasundaram G, Sato M, Webster TJ (2006) Biomaterials 27:2798
28. Rusu VM, Ng CH, Wilke M, Tiersch B, Fratzl P, Peter MG (2005) Biomaterials 26:5414
29. Rochas C, Rinaudo M, Landry S (1990) Carbohyd Polym 12:255
30. Macartain P, Jacquier JC, Dawson KA (2003) Carbohyd Polym 53:395
31. Sachlos E, Czernuszka JT (2003) Eur Cell Mater 5:29
32. Chen G, Ushida T, Tateishi T (2002) Macromol Biosci 2:67
33. Danilchenko SN, Kukharenko OG, Moseke C, Protsenko IY, Sukhodub LF, Sulkio-Cleff B (2002) Cryst Res Technol 37:1234
34. Landi E, Tampieri A, Celotti G, Sprio S (2000) J Eur Ceram Soc 20:2377
35. Gibson LJ, Ashby MF (1997) In: Cellular solids: structure and properties. Cambridge University Press, Cambridge
36. Verheyen CCPM, de Wijn JR, van Blitterswijk CA, de Groot K (1992) J Biomed Mater Res 26:1277
37. Elliot JC (1994) In: Structure and chemistry of the apatites and other calcium orthophosphates: studies in inorganic chemistry, vol 18. Elsevier, Amsterdam, pp 43–44
38. Rey C, Frèche M, Heughebaert M, Heughebaert JC, Lacout JL, Lebugle A, Szilagyi J, Vignoles M (1991) Bioceramics 4:57
39. Zhang X, Li Y, Lv G, Zuo Y, Mu Y (2006) Polym Degrad Stabil 91:1202
40. Liao C-J, Lin F-H, Chen K-S, Sun J-S (1999) Biomaterials 20:1807

41. Prado-Fernandez J, Rodriguez-Vazquez JA, Tojo E, Andrade JM (2003) Anal Chim Acta 480:23
42. Andersson J, Areva S, Spliethoff B, Lindén M (2005) Biomaterials 26:6827
43. Krylova E, Ivanov A, Orlovski V, El-Registan G, Barinov SJ (2002) Mater Sci-Mater M 13:87
44. Perrin FX, Nguyen V, Vernet JL (2003) J Sol-Gel Sci Techn 28:205
45. Dorozhkin SV, Epple M (2002) Angew Chem Int Ed 41:3130
46. Gutowska A, Jeong B, Jasionowski M (2001) Anat Rec Part A 263:342
47. Zhang W, Piculell L, Nilsson S, Knutsen SH (1994) Carbohyd Polym 23:105
48. Hikichi K (1993) Polym Gels Networks 1:19
49. Hammond C (2001) In: The basis of crystallography and diffraction, 2nd edn. Oxford University Press, Oxford
50. Zhang R, Ma PX (1999) J Biomed Mater Res A 44:446
51. Tampieri A, Celotti G, Landi E (2005) Anal Bioanal Chem 381:568
52. Klein CPAT, Driessen AA, de Groot K, van den Hoof A (1983) J Biomed Mater Res 17:769
53. Knoack D, Goad MEP, Aiolova M, Rey C, Tofighi A, Chakravarthy P, Lee DD (1998) J Biomed Mater Res B 43:399
54. Athanasiou KA, Zhu C-F, Lanctot DR, Agrawal CM, Wang X (2000) Tissue Eng 6:361
55. Yaszemski MJ, Payne RG, Hayes WC, Langer R, Mikos AG (1996) Biomaterials 17:175
56. Jing R, Hongfei H (2001) Eur Polym J 37:2413